

Supporting Information

Bethel and Grabe 10.1073/pnas.1607574113

SI Materials and Methods

Continuum Calculations. Continuum membrane-bending calculations were carried out as described in refs. 15–17. Briefly, a physics-based model is used that considers the energy of the protein in the membrane as the sum of three dominant terms:

$$G^T = G^{(e)} + G^{(np)} + G^{(me)}, \quad [\text{S1}]$$

where $G^{(e)}$ is the electrostatic energy, $G^{(np)}$ is the nonpolar energy, and $G^{(me)}$ is the membrane deformation energy. The membrane deformation and its associated energy are determined by prescribing displacement and contact angle boundary conditions and solving the Euler–Lagrange equation that comes from a Helfrich-like energy functional (16, 43). The electrostatic energy is calculated by solving the Poisson–Boltzmann equation using the software package APBS (adaptive Poisson–Boltzmann solver) (49). The nonpolar energy associated with burying portions of the protein in the water-excluded regions of the membrane is assumed to be proportional to the protein’s buried solvent-accessible surface area (SASA):

$$G^{(np)} = a \cdot (A_{mem} - A_{sol}), \quad [\text{S2}]$$

where A_{mem} is the SASA of the protein in the membrane, A_{sol} is SASA of the full protein before membrane insertion, and a is a surface tension ($0.028 \text{ kcal/mol} \cdot \text{Å}^2$) (15, 26, 49). The displacement and contact angle boundary conditions that minimize G^T are determined by optimization starting with a global simulated-annealing method followed by local optimization with Powell’s method (16, 51). All continuum membrane surfaces are the final minimized results computed using the 3.3 Å X-ray structure of nhTMEM16 (PDB ID code 4WIS) or homology models based on 4WIS.

MD Methods and Analysis. Eight independent simulations of system 1 and eight of system 2 were equilibrated using the default equilibration scheme provided by CHARMM-GUI for a total 5.075 ns. The last step of equilibration was extended by 4.8 ns with no restraints on the membrane, but a $0.1 \text{ kcal/mol} \cdot \text{Å}^2$ restraint on the protein backbone heavy atoms to allow the

membrane to relax around the protein before production runs. For production, simulations were run using a semiisotropic pressure tensor and the Berendsen barostat. The Langevin thermostat was used with a temperature setting of 303.15 K and a friction coefficient of 1 ps^{-1} . The SHAKE algorithm was used with a 2-fs time step. A nonbonded cutoff of 8 Å was used and electrostatics were calculated using the particle mesh Ewald method. Two additional simulations were initiated starting from production snapshots from systems 1 and 2 in which a single POPC lipid in the hydrophilic groove was replaced by a POPS lipid. Because the lipid tails of POPS and POPC are identical, only the headgroups were replaced. These systems were equilibrated using the default scheme from CHARMM-GUI for 375 ps, followed by 100 ns of production for each.

Representative membrane surfaces from the MD simulations were calculated by averaging membrane configurations at a 0.2-ps stride as follows. Each snapshot was aligned to the starting structure at time 0 by first centering the transmembrane domain of the protein and then rotating the system about the z axis to minimize the root-mean-squared deviation of the transmembrane domain backbone atoms. We only allowed rotations about the z axis to prevent out of plane rotation of the membrane from frame to frame. For each snapshot, we constructed the upper and lower surfaces where the headgroups meet the lipid tails by considering the collection of C2 carbon atoms of the phospholipid acyl chains. The space between these surfaces defines the hydrophobic core of the membrane. Interpolated surfaces for the upper and lower leaflets were generated using the cubic interpolation function available in SciPy (51). To determine the phosphorus densities in Fig. 2, we followed the same alignment procedure and then binned on the phosphorus positions using a 3D Cartesian array with 2 Å spacing. The reported density was averaged over all snapshots. The dipole vector field was calculated by taking snapshots from all simulations using 1-ns spacing. We aligned the helices forming the hydrophilic groove then binned lipid headgroups in 3D space and averaged their dipole vector in each bin. Bins with less than 20 lipids were omitted due to poor sampling.

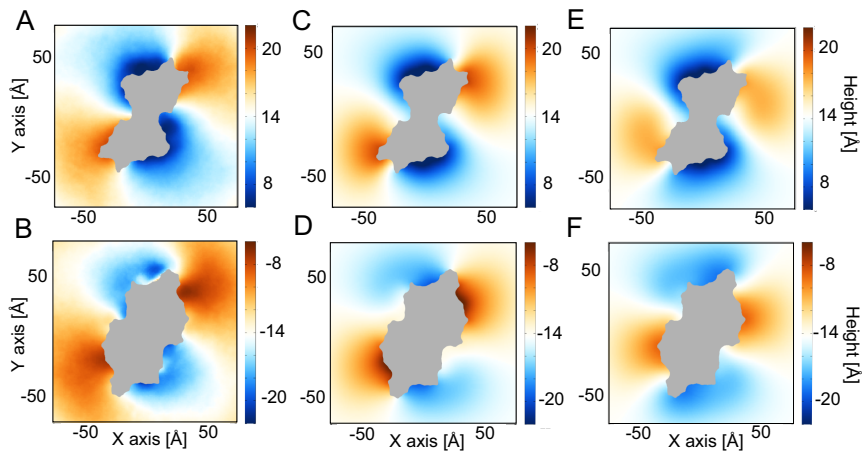


Fig. S1. Extracellular view of upper and lower leaflet heights predicted from MD and continuum calculations. (*A* and *B*) The upper and lower leaflet surfaces, respectively, calculated from averaging results from MD simulations. (*C* and *D*) The upper and lower leaflet surfaces, respectively, determined from continuum calculations. (*E* and *F*) The upper and lower leaflet surfaces, respectively, determined from continuum calculations when all residues within the hydrophilic groove are neutralized. Surfaces are colored by height, where red is an upward deflection, blue is a downward deflection, and white is no deflection. The area occupied by the protein is shaded gray.

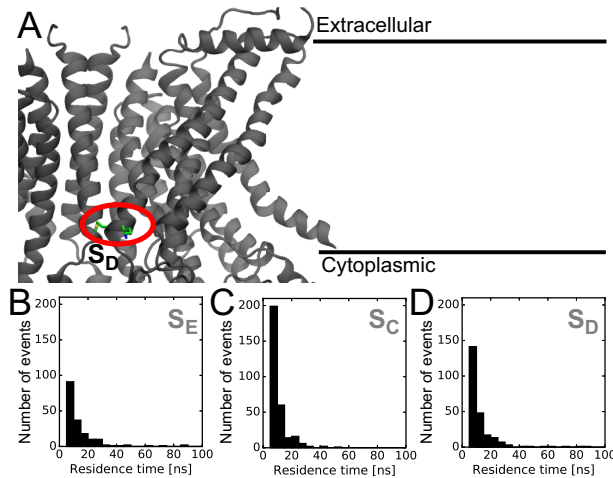


Fig. S2. Residence times of lipid-binding sites compared with control site. (*A*) Residues forming the dummy site S_D used as a control in the residence time calculations. The methionine and lysine forming this site are circled in red. (*B–D*) Residence times of lipid headgroups at the S_E , S_C , and a control S_D site, respectively. Two outlier residence times of 248 and 317 ns were omitted from *B*.

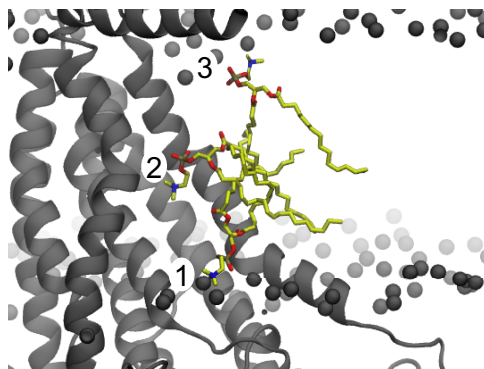


Fig. S3. Phospholipid configurations during a flopping event where 1, 2, and 3 are early, middle, and late in the processes, respectively. TM3 and TM4 were removed for clarity.

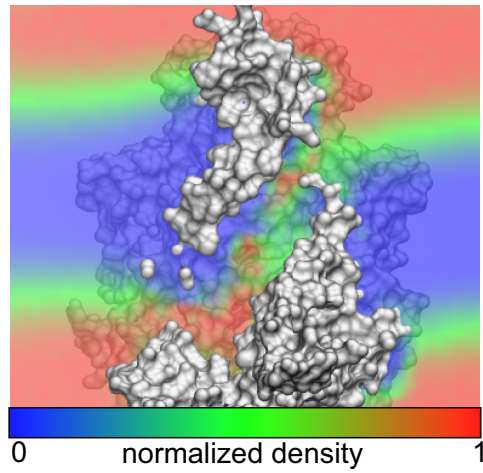


Fig. S4. Cross-section of normalized water density overlaid on nhTMEM16 structure. Water enters the hydrophilic groove achieving densities close to bulk values (red) at several locations.

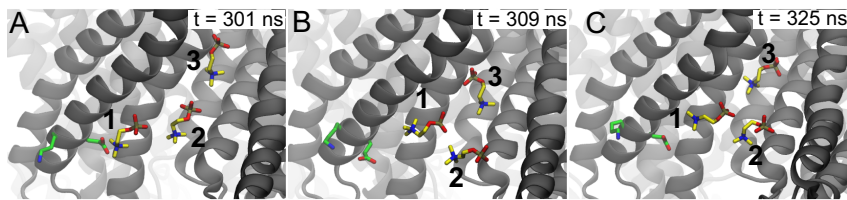


Fig. S5. Atomic details of lipid flipping. A–C are sequential MD snapshots showing dipole stacking during a lipid-flipping event. Before A, lipid 3 crossed the narrow portion of the groove from the S_E site to add itself to the top of the dipole stack already composed of lipids 1 and 2. In B, lipid 2 dissolves from the stack, and then in C, lipid 3 forms a new dipole interaction with lipid 1, resulting in a shorter stack. These interactions closely resemble the time-reversed stacking interactions seen during the lipid-flipping events (Fig. 4).

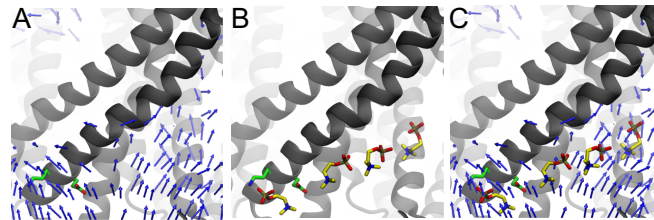


Fig. S6. Lipid dipoles align near S_C site. (A) Three-dimensional vector field of PC lipid dipoles at the cytoplasmic end of the hydrophilic groove. Arrows point from the positive to the negative charge. (B) Dipole lipid stack from the S_C . This snapshot is from a simulation where a lipid did not fully permeate. (C) Dipole stack superimposed on the 3D dipole vector field.

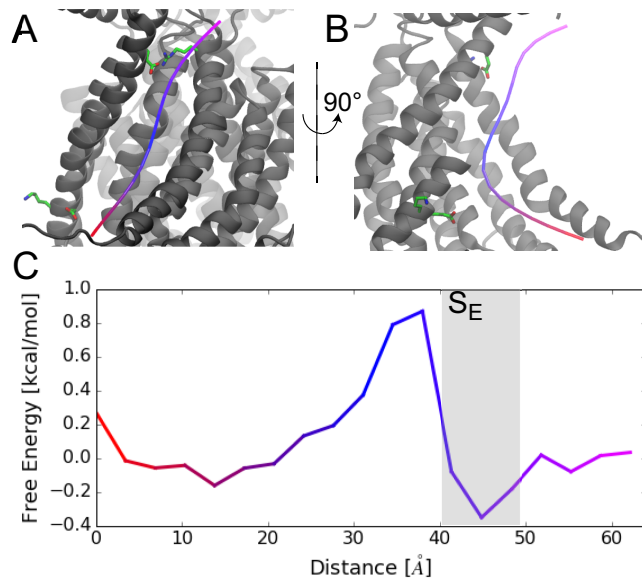


Fig. S7. Permeating lipids experience a small energy barrier. (A) Minimum-energy pathway through the hydrophilic groove determined using a string method. (B) Rotated view of the minimum-energy path. The extracellular half of TM4 is removed for clarity. (C) Free-energy profile along the minimum energy path. The color scheme matches the coloring of the path in A and B.

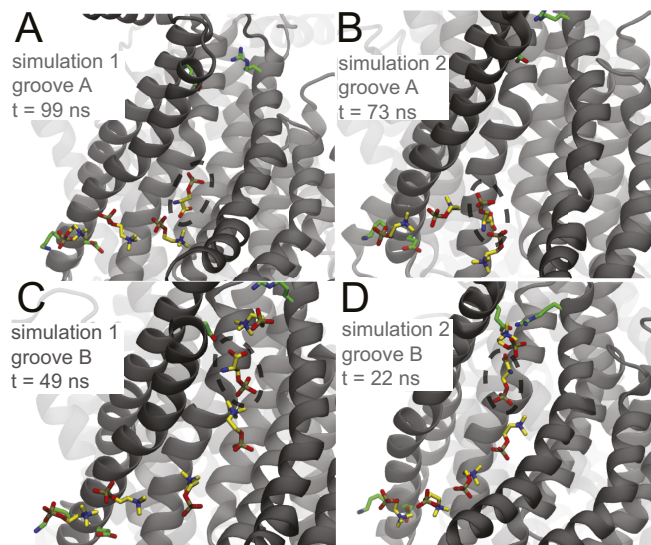


Fig. S8. POPC dipole stacking stabilizes POPS in the hydrophilic groove. Single PC headgroups were replaced with PS (indicated by dashed circles) and restarted for two simulations (two grooves per simulation; four POPS lipids total). Two POPS molecules were placed in the cytoplasmic side of the groove (A and B), and two were placed in the extracellular end (C and D). Simulations were run for 80 ns, and the snapshots were taken at different times after 20 ns of production. Dipole stacks were observed in all four hydrophilic grooves. For C and D, the dipole stacks observed were not present at the beginning of the simulations. Interestingly in B, when POPS in the middle of the dipole chain, the PC dipoles switch directions, as expected. This result could have an important consequence on lipid flipping through the midplane barrier.

```

nhTMEM16  -GVD--FVIVHYKVPAAE-----RDEAEAGFVQLIRALTTVGLATEVRHGE--NESLLVFVKVA
hsTMEM16F  RRTD--FVLVYDESRKET-----NKKGTNEKQRRKRQAYESNLICHGLQLEATRSVLDDKLVFVKVHAP
hsTMEM16A  RKVD--YILVYHHKRPSGNRTLVRVQHSSTPSGARSVKQDHPLPGKGASLDAGSGEPPMDYHEDDKRFRREEYEGNLEAGLELERDEDTKIHGVGVFKIHAP
hsTMEM16K  SSFTPLVVIELAQDVKEET-----KEWLKNRIIAKKKDGAQLLFRPLLNKYEQET--LENQNLVYLGAS

nhTMEM16  SPDLFAKQVYRARLGDWLHGV-----RVS----APHNDI-AQALOQEPVVEAERLRLIYLMLITPHN--
hsTMEM16F  -WEVLCTYAEIMHIKLPKPNDLKRRSSAFGTL-----NWFTKVLVDE-SIKPEQEFTTAPFEKRRMDFY--IVDRDAFFNPATRSRIVYFVILSRVKYQV
hsTMEM16A  -WNVLCREAEFLKLMPTKK-MYHINETRGLLKKINSVQLKITDPIQPKVAEHRPQTMKRLSYFPRSREKQHLFD--LSDKSFDFSKTRSTIVYELKRTCTFK
hsTMEM16K  -KIRMLLGAEAVGLVKECND-----NTMRAFTYRTRONPKGFDDNDDFLTMAECQPIIKHELENLRAKD

nhTMEM16  -----EWKHVESIFPLHSH-----SFNKEWIKKWSK-YTLEQTDIDNIRDKFGESVAFYFAFLRSYFRFLVIPSAFCF
hsTMEM16F  IN-----NVSKFGINRLVNSGIYKAAPLHDCKFRQSEDPSCPNERYLLYREWAHPRSIYKKQPLDLIRKYYGEKIGIYFAWLGYYTQMLLLAAVVG
hsTMEM16A  A-----KYSMGITSLLANGVYAAAYPLHDGDYNGEN--VEFNDRKLLYEAWARYGVFYKYQPIDLVRKYFGEKIGLYFAWLGYYTQMLIPASIVCI
hsTMEM16K  EKMIPGYPQAKLYPGKSLRRLTSGIIVQVPLHDS-----EALKKLEDTYTR-FALKYQPIDSRGYPGETTALYFGLEYFTFALIPMAVIGL

nhTMEM16  GAWLLLG-----QFSYLYALLCGLWSVVFYEWKQEVDLAVQWGVGRVSSIQ-----
hsTMEM16F  ACFLYGYLNQDNTWSKEVCHPDIGGKIIMCPQCRLCPFWKLNITCESKRLCIFDSFGTLVFAVFMGVVVTFLFEFWKRRQALEYEDWTVELQOEE-----
hsTMEM16A  IVFLYGCATMDENIPMEMCDQR--HNITMCLCDKTCYWKMSACATARASHLFDNPATVFFSVFMAWAAFTMEHWKRRKQMLRNLRYRDLTGFEEEEAVKD
hsTMEM16K  PYLFLVVE-----DYDKYVIFASNLINLSTVILELWKKRCANMTYRWGTLMLKRKF----E

nhTMEM16  QSRPEFEWEH--EAEDEPI-----TGE-PVKVY-PPMKRVKTQLL-QIPFALACVVALGALIVTCNSLEVFINEVYSG-----
hsTMEM16F  QARPEYEAARCHVIVINEI-----TOE-EERTPPTAWGKCIRITL-CASAVFWILLIIASVIGIIVYRLSVFVFSAKLPKN
hsTMEM16A  HPRAEYEARVLEKSLKESRNKEKRRHIPEESTNKWKQRVKTAMAGVLTDKVKTWRDRFPAYLT-NLVSIIIFMIAVTFIIVLGVIIYRISMAALAMNS---
hsTMEM16K  EPRPGFHGV--LGINSI-----TGK-EEPLY-PSYKROLRIYLVSLPFCVCLLYFSLYVMMIYFDMEVWALGLHENS---

nhTMEM16  -----PGKQYLGFLPTLFLVIGTPTISGVLMGAAEKLNAMENYATVDAHDAALIQQFVLFNFMYSYALFFTAFFVYIPFGHILHPLNFWRATAQTLT
hsTMEM16F  INGTDPIQKYLTPQATSTASTISFTIIMILNTIYEKVAIMITNFELPRTQTDYENSLTMKMLFPQFVNYSSCFYIAPFKGKFGVGPDPVYWLKGYRNE--
hsTMEM16A  -----SPSVRSNIRVTVTATAVILNLVVIILLDEVYGCIARWLTKIEVPKTEKSFEEELIFKAFLLKFNVSYPPIFYVAFKGRFVGRPGDVYVIFRSFRME--
hsTMEM16K  -----GSEWTSVLLYVPSIIYAVIETMNRLYRYAAEFLTSWENHRLESAYQNHILKVLVFNFLNCFASLFIYAVLKD-----

nhTMEM16  FSEKELPTREFQINPARISNOMFYFTVTAQI-VNFATVAVVYIKQAFQAEF-----LQVRRECTLE-EYDVSQDYREVMVMOFGYVAMFS
hsTMEM16F  -----ECDPGCCLLELTTQLTIIIMGGKAL-WNNIQVLLLEWIMNLIGRFRVSGSE-----KITPRWEQDYHLQPMG-KLGLFYEYLEMIIQFGFVTLFV
hsTMEM16A  -----ECAPGGCMLMELCIQLSIIIMLGKLIQNNLFIIGIPKMKKLIYRLKQKQSPDHEECVKKRQRYEVDYNLEPF---AGLTPEYMEMIIOFGFVTLFV
hsTMEM16K  -----MKLLRQSLATLLITSQI-LNQIMESFLEYWLQKRGVVRKRVQALK--ADIDATLYEQVILEKEMGTYLGTFFDYLFLQFGYVLSLFS

nhTMEM16  VAWPLAACFLVNNWVELRSDALKIAISSREPIPWRTDSIGPWLTALESLSWLGSISSAIVYLCSNASPLKA-----
hsTMEM16F  ASFPLAPLLALVNNILEIRVDAWKLTQFRRLVPEKAQDIGAQPIMQGAILAVVTNAMIIFTSDMIPRLVYYSFVSPYPGDHSTYMEGYINNTLSIFKV
hsTMEM16A  ASFPLAPLALLNIIIEIRLDAKFKVTELREPVAVRADIGIWIYNILRGIGKLAVIINAFVISFTSDFIPRLVLYMYSK-----NGTMHGFVNHTLSSFN
hsTMEM16K  CVYPLAAAFVLLNFTVNSDALKMCRVFKKPFSEPSANIGVWQLAFETMSVIVSVTNCALIGMSPQVNAVF-----

nhTMEM16  -----WGLLLSILFAEHFYLIVQLAVRFVLSKLDSPGLQEKERERFQTKRRLLENLGQDAA
hsTMEM16F  ADFKNKSKGNPY-SDLGNHTTCRYRDFRYPGHPQEQYKHNIYVHVIAAKLAFIIVMEHVIYSVKFFISYAIPDVSKRTKSKIQREKYLTKQLLHENHLKDMTK
hsTMEM16A  SDFQNGTAPNDPLDLGYEVQICRYKDYREPPWSENKYDISKDFWAVLAARLAFVIVFQNLVFMMSDFVDWVDPIDPKDISQIHKVLMVELFMREEQDKQQL
hsTMEM16K  -----PES--KADLILIVVAVEHALLALKFI LAFATPDKPRHIQMKLARLEFESLEALKQOQMKLVTE--

nhTMEM16  AAPGIE----HSEKITREALEEEARQASIEFWQRQ-----MQETIEIGRRMIEQQL---AAG
hsTMEM16F  NMGVIAERMIE-----AVD--NNLRPKSE-----
hsTMEM16A  -LETWMEKERQ-----KDEPPCNHHNTKACPDS-LGSPAPSHAYHG-GVL---
hsTMEM16K  NLKEEPMESGK--EKAT-----

```

Fig. S9. Sequence alignment of TMEM16A, TMEM16F, TMEM16K, and nhTMEM16. This alignment was carried out with the program Promals3d (47) using all 10 human TMEM16 family members plus nhTMEM16. No hand adjustments were performed. Strictly conserved residues are highlighted green and homologous residues are yellow.

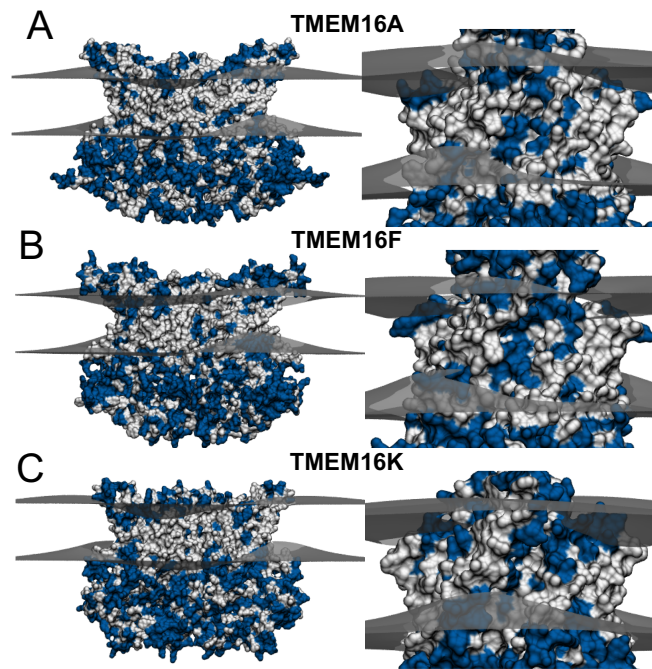
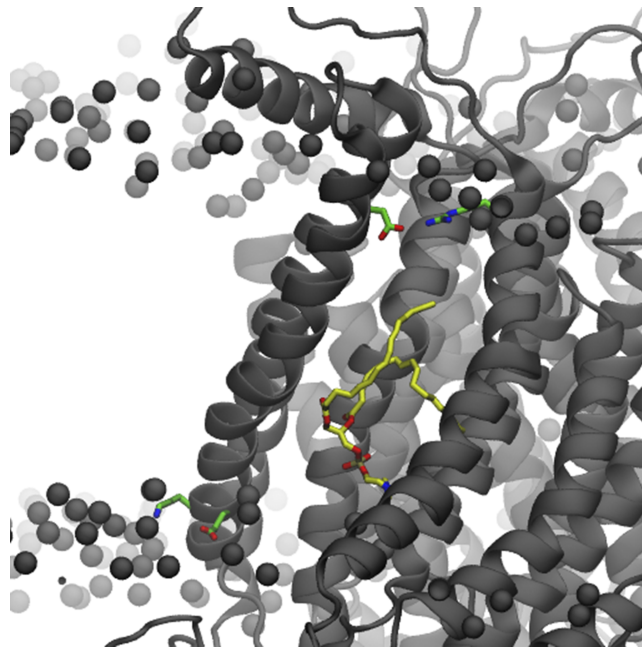


Fig. S10. Predicted membrane deformations around mammalian TMEM16 family members based on continuum modeling: TMEM16A (A), TMEM16F (B), and TMEM16K (C). Ninety-degree rotations of each protein showing the hydrophilic groove are displayed to the right. The predicted membrane surfaces at the upper and lower hydrophobic–hydrophilic interfaces are gray. Hydrophobic and hydrophilic residues on the proteins are white and blue, respectively.

Table S1. Parameter values used in all continuum model calculations

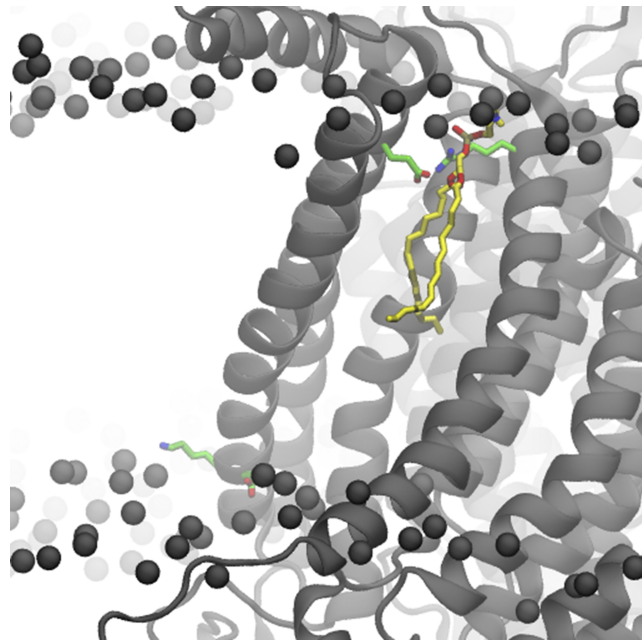
Parameter	Value	Ref(s).
Membrane thickness (L_0)	28.5 Å	18
Surface tension (α)	3.00×10^{-13} NÅ	19
Bending modulus (K_c)	8.5×10^{-10} NÅ	20
Gaussian modulus (K_G)	$\sim -0.9 \times K_c$	21, 22
Compression modulus (K_a)	2.13×10^{-11} NÅ	23, 24
Partenskii–Jordan coefficient	4.27	17, 25
Protein dielectric (ϵ_p)	2.0	26
Membrane core dielectric (ϵ_{hc})	2.0	27
Headgroup dielectric (ϵ_{hg})	80.0	27
Water dielectric (ϵ_w)	80.0	26

All membrane values correspond to POPC bilayers. Additional parameters used in the electrostatic calculations are identical to values reported in ref. 19.



Movie S1. Full lipid-flipping event during 120-ns MD simulation. The POPC lipid (yellow) starts in the cytoplasmic leaflet near the protein. Between 40 and 60 ns, the lipid interacts with the hydrophilic groove of nhTMEM16 to traverse the bilayer and enter the extracellular leaflet. All other lipid headgroups are represented as gray spheres. The protein (gray) is drawn in cartoon representation. The residues forming the SC and SE sites are shown in green. Waters are omitted for clarity.

[Movie S1](#)



Movie S2. Full lipid-flipping event during 400-ns MD simulation. The POPC lipid (yellow) starts in the cytoplasmic leaflet near the protein. Between 280 and 320 ns, it interacts with the hydrophilic groove of nhTMEM16 to traverse the bilayer and enter the cytoplasmic leaflet. All other lipid headgroups are represented as gray spheres. The protein (gray) is drawn in cartoon representation. The residues forming the SC and SE sites are shown in green. Waters are omitted for clarity.

[Movie S2](#)